A transition loss theory for waves reflected and transmitted by an overwashed body

David M. Skene and Luke G. Bennetts

University of Adelaide, Adelaide, SA 5005, Australia

May 23, 2021

Abstract

A transition loss theory for waves reflected by an overwashed step and transmitted by an overwashed plate is presented. The theory is based on a conservation of energy technique to correct the transmission/reflection predicted by linear potential flow theory by taking into account the energy flux into the overwash and the mechanical energy dissipated by the formation of overwash. Wave energy dissipation is calculated by assuming that the transition from deep water to shallow water flow occurs over a sufficiently narrow domain such that it can be modelled as a discontinuity in the flow (akin to a hydraulic jump). Theoretical predictions are compared to CFD model data for the step problem and laboratory experimental measurements for the plate problem. Generally excellent agreement is found for all cases tested, and the theory gives significant improvements compared to linear models that do not capture overwash effects and a theory that does not account for energy loss in the transition domain.

1 Introduction

It is common to model interactions between surface water waves and bodies (fixed, floating, submerged, etc.) using linear potential flow theory [18], as it is then possible to apply powerful mathematical solution methods that generate highly accurate approximations at low computational costs [13]. Linearity requires all motions to be small perturbations from the equilibrium state such that the problem can be posed on a fixed water domain [18]. However, linear conditions may not hold, even for low steepness incident waves and small body motions, when the body is submerged but very close to the free surface, such as breakwaters [23], reefs/shelves [10], and submerged wave energy converters [16], or has a small freeboard, such as sea ice floes [15, 7]. In these situations, mild (i.e. low steepness) incident waves may create a shallow-water flow on top of the body, involving an abrupt increase the free surface steepness. In the sea ice literature, the phenomenon is known as overwash [3]. Overwash contrasts with green water, in which extreme waves break over the upper surface of a large freeboard body, such as an offshore vessel [31, 9, 8, 5].

Overwash has been observed in wave tank experiments on small freeboard bodies, typically being used to model sea ice floes [26, 19, 7]. The experiments mostly involve solitary thin (elastic) plates subjected to regular incident waves in the regime where wavelengths are comparable to the plate length (the scattering regime, where wavelength to plate length ratios are approximately order 1 [20]). In this wave regime the plate reflects some of the incident wave energy and therefore only transmits a portion of the incident wave beyond the plate. The reflection/transmission problem can be modelled using linear potential theory, which conserves energy, but this method cannot take into account phenomenon of overwash when the incident waves are sufficiently large such that they produce a free surface that exceeds the plate's freeboard. When overwash does form, it is characterised by turbulent bores on the plate, along with collisions between bores travelling in opposite directions when large incident amplitude waves generate overwash at both leading and trailing ends of the plate [24].

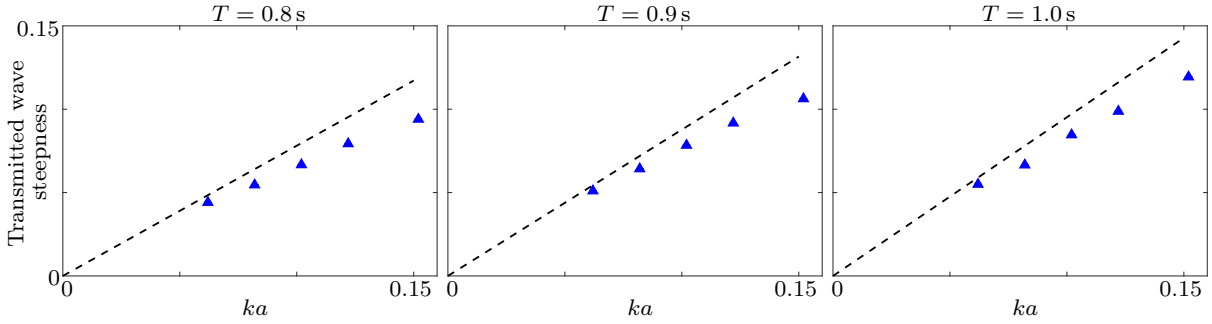

Figure 1: Steepness of waves transmitted by an overwashed plate versus incident wave steepness, as measured in wave tank experiments (blue symbols), and predicted by linear potential-flow theory (dashed black curves); adapted from Fig. 13 of [21].

The occurrence of overwash is linked to reduced amplitudes of body motions [17, 29] and lower energy in the transmitted waves than predicted by linear potential-flow theory [1, 3, 28, 21]. Toffoli et al. [28] and Nelli et al. [21] analyse measurements from tests on plates with an edge barrier (to suppress overwash) and without an edge barrier (to allow overwash). They find linear potential-flow theory accurately predicts transmitted wave amplitudes when overwash is suppressed, but significantly over-predicts transmitted amplitudes when overwash is allowed; noting the transmitted amplitude for an individual ice floe is used to predict wave energy attenuation in the sea ice covered ocean [2]. Figure 1 is adapted from [21], and shows the over-prediction in terms of transmitted wave steepness versus incident wave steepness. It demonstrates that the transmitted wave over-prediction increases with increasing incident steepness in a sublinear trend, and, hence, linear potential-flow theory predictions become increasingly inaccurate with increasing overwash depth and velocity. Further, [28] and [21] also find the reflected wave amplitude is insensitive to overwash, and conclude the reduced transmission is caused by energy dissipation in the overwash, identifying the turbulent bores and bore collisions as the most likely sources of energy dissipation.

Skene et al. [24] propose a mathematical model for overwash on a floating elastic plate, in which the domain is decomposed into the overwashed water, which is modelled using nonlinear shallow water theory, and the surrounding (deep) water and plate, which are modelled by coupled linear potential-flow and thin plate theories. In the model, overwash is forced without considering how it affects the surrounding waves, i.e. a 'one way coupling' is used. They compare the model with wave tank experiments, and show it predicts overwash properties (depths and bore speeds) accurately up to the point bore collisions occur, which generally start to occur for incident wave steepnesses above 0.08, and are more likely to occur for wavelengths less than the plate length. Skene et al. [25] apply the model to the simpler problem of overwash of a rectangular zero-draft step (see figure 2), in which bores are generated at one location only and hence do not collide. They compare the model to results given by a two-phase Navier–Stokes computational fluid dynamics (CFD) model, and show it predicts overwash depths and velocities accurately after a relatively short distance along the upper surface of the step, despite not capturing these quantities at near the step vertex where wave breaking occurs. They attribute the transition to accuracy to the mathematical model capturing the overwash energy and mass flux at all locations along the step, including at the step vertex.

Up to this point, only CFD techniques have been used to model waves surrounding (reflected and/or transmitted by) an overwashed body. Nelli et al. [22] and Huang et al. [11] model the experiments of [21], using the two-phase Navier-Stokes equations, where [22] assume a rigid plate, but [11] use a CFD model that includes solid deformation and two-way fluid–structure interactions, which can account for the elasticity of longer plates. In a differing CFD approach, [30] use smoothed particle hydrodynamics to model the experiments of [22]. The CFD models closely match the experimental measurements

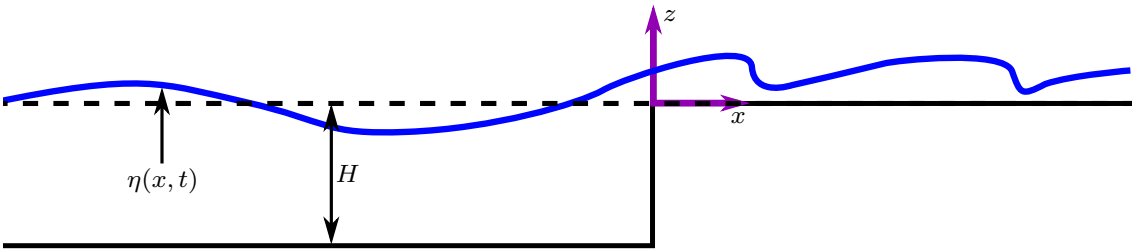

Figure 2: Schematic of the step problem (not to scale).

with regard to the overwash on the plate and the transmitted waves. Moreover, Nelli et al. [22] find a high level of energy dissipation in the overwash and around the plate's edges.

This paper introduces a transition-loss theory to predict reflected/transmitted wave amplitudes around an overwashed body. The CFD model of [25] is used to analyse the waves reflected by an overwashed step (noting that reflection analysis was not conducted by [25]). The reflected waves are shown to be similar linear potential-flow predictions with respect to phase and frequency, but, similar to the waves transmitted by an overwashed plate, have significantly smaller amplitudes. A transition-loss theory is proposed to capture the reduced reflection of the overwashed step. The theory is based on a conservation of energy technique that accounts for energy flux into the overwash and energy dissipated by overwash formation. It uses the mathematical overwash model [25], which does not model the affects of overwash on the reflected waves. The transition-loss theory does not require input from the CFD model, is computationally efficient, and shows strong agreement with the reflected waves extracted from the CFD data. The transition-loss theory is extended to the more challenging problem of predicting the amplitudes of waves transmitted by a floating elastic plate. Similar to the step problem, the transition-loss theory for the plate problem builds on the mathematical overwash model of [24] (which does not model the affects of overwash on the transmitted waves), is computationally efficient (i.e. does not require CFD modelling), and shows strong agreement with transmitted wave amplitudes measured in experimental tests.

2 Reflection by a step

2.1 Problem description

Consider a two dimensional wave basin filled to a depth of $H = 1\,\mathrm{m}$. Define positions in the basin using the Cartesian coordinate system (x,z), where the z-direction points upwards and the x-direction points along the still water line. Locate a step (sheer vertical wall) at $x = 0$ and let the step have an upper surface level with the still water line for $x > 0$. Let the step be subject to incident waves generated at $x \ll 0$, which drive overwash on the step. Let the incident waves be regular, with frequency ω and steepness ka, where a is the wave amplitude, and k is the wave-number given by the dispersion relation $k\tanh(kH) = \omega^2 g^{-1}$, where $g = 9.81\,\mathrm{m\,s^{-2}}$ is gravitational acceleration. Allow the basin to be effectively infinite in length, such that waves can radiate out freely in the positive and negative x-directions. Figure 2 shows a representative schematic of the problem.

2.2 CFD reflection analysis

The CFD model from [25] is used to analyse the waves reflected by the step, and the reflected amplitudes extracted from the CFD data are used to validate the transition-loss theory to be developed in

§2.5. The technical details for the CFD model of the step have been presented in [25] and hence only its important inputs/outputs for analysing the waves reflected by the step are recounted here. The CFD model uses a virtual wave-maker located at $x = -10\,\mathrm{m}$. It generates incident waves of angular frequency $\omega = 6.41$, 7.85, and $10.5\,\mathrm{rad\,s^{-1}}$, with each frequency run for steepnesses $ka = 0.03$, 0.06, 0.1 and 0.13. Simulations are run using both slip and no-slip conditions on the surface of the step, noting that the condition type affects overwash depths and speeds [25]. Free surface signals, $\eta(x,t)$, are measured to determine the reflected waves for $0 < t < 28\,\mathrm{s}$ at all locations to the left of the step ($x < 0$). Qualitatively, the non-dimensional free surfaces, $\eta(x,t)/a$, were found to be similar for all incident wave frequencies tested. Therefore, for the sake of brevity, the tests presented and analysed in this work use only incident waves with period $T = 2\pi\omega^{-1} = 0.8\,\mathrm{s}$ (wavelength $\lambda = 2\pi k^{-1} = 1.0\,\mathrm{m}$), and amplitudes $a = 5$, 10, 15, and 20 mm.

Figure 3 shows the free surface signal at $x = -2.00\,\mathrm{m}$ over the duration of the $a = 15\,\mathrm{mm}$ simulation for the no-slip boundary condition (blue) and slip boundary condition (dashed teal). The slip and no-slip boundary conditions match almost exactly at all times. This indicates the basin's boundary conditions do not affect the waves reflected by the step even though they affect the overwash properties. This result holds for all incident wave conditions tested. As a consequence, all future discussion will more refer to the no-slip case only.

The black, vertical lines on figure 3 indicate three distinct stages of the simulation. Between $t = 0$ and $t = 7\,\mathrm{s}$, incident waves build up at the measurement location and reach the target amplitude and frequency. Between $t = 7\,\mathrm{s}$ and $t = 21\,\mathrm{s}$, the waves reflected by the step enter the measurement location, and, as the reflected waves are growing in magnitude, the free surface is in a transient state. Between $t = 21\,\mathrm{s}$ and $t = 28\,\mathrm{s}$, the wave field reaches a periodic state, notwithstanding the gradual decline in the peaks and troughs of the signal, which is due to net advection of water onto the step slightly reducing the equilibrium depth of the water in the basin. The reflection coefficient is extracted from the interval in which the wave field is periodic.

Figure 4 shows the free surface signal for $21 < t < 25\,\mathrm{s}$ at measurement locations $x = -2.00$, -1.75, and $-1.50\,\mathrm{m}$. Results are shown for the step simulation where overwash occurs (solid blue), and a simulation where the step height has been increased such that no overwash occurs (dashed black). For the no overwash case, the plots show that at $x = -2.00\,\mathrm{m}$ and $x = -1.50\,\mathrm{m}$, the free surface oscillates with amplitude $2a$ and at $x = -1.75\,\mathrm{m}$ the free surface is stationary. Therefore, considering that the incident wavelength is $\lambda = 1\,\mathrm{m}$, the results indicate the raised step produces a standing wave field, which is consistent with linear potential-flow theory (the standing wave result has been known as far back as [12] §9).

For the case where overwash occurs, at $x = -2.00$ and $-1.50\,\mathrm{m}$ the free surface oscillates at the same frequency as the incident wave, but with a reduced amplitude (relative to the test without overwash) of $\approx 1.75a$. The signals at these two points are almost exact reflections about the $t = 0$ line. This suggests the wave field is dominated by an incident and reflected wave at the same frequency and phase of the incident wave, but with a reduced reflected wave amplitude due to the overwash; i.e. $\eta(x,t) = a\cos(\omega t - kx) + r\cos(\omega t + kx)$ with $r < a$. Nonetheless, the signal at $x = -1.75\,\mathrm{m}$ displays two peaks and troughs per incident wave period, which indicates the presence of higher-order (with respect to wave frequency) harmonics in the reflected wave field.

The wave field is decomposed into incident and reflected components, using the three point probe technique devised by [14]. The technique assumes the wave field is made up of a spectrum of linear incident and reflected waves. It separates them by applying the fast Fourier transform (FFT) to three closely located free surface probes (further details can be found in [14]). Conventionally, the method is used to extract incident and reflected energy spectra, but it can be adapted to give spectral amplitudes and phases. A free surface sampling window $21 < t < 27.4\,\mathrm{s}$ is used for the analysis. This window is chosen such that its length is an integer multiple of the incident wave period, thus centring the FFT frequency bins at the incident wave frequency and minimising spectral leakage. The method is applied to probe arrays at $x = -2.00$, -1.90, and $-1.88\,\mathrm{m}$, and $x = -0.40$, -0.30, and $-0.20\,\mathrm{m}$. The far field

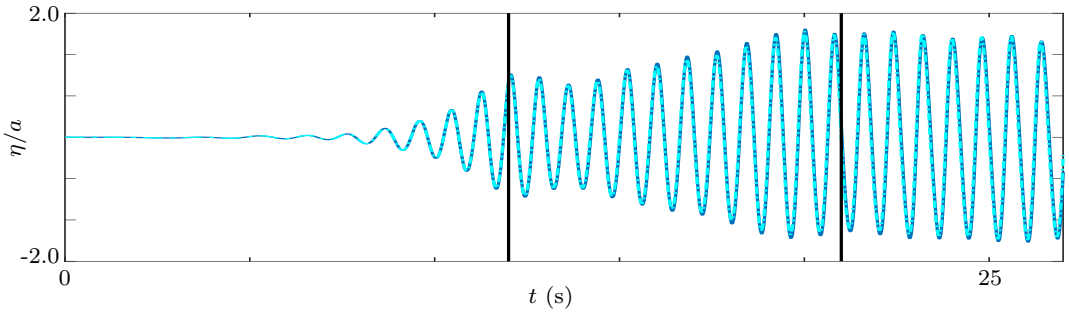

Figure 3: CFD free surface signals at $x = -2.00\,\mathrm{m}$ for step problem over the entire simulation duration, for incident wave period $T = 0.8\,\mathrm{s}$ and amplitude $a = 15\,\mathrm{mm}$. Results are shown for simulations with slip (solid blue) and no-slip (dot dashed teal) basin boundary conditions.

array is used to measure the reflected waves and the near field array is used to determine if the flow properties change near the step vertex.

Figure 5 shows the reflected wave steepness at the fundamental frequency (kr) as a function of the incident wave steepness. Results are given for the higher step that experiences no overwash (dashed black) and the lower step that experiences overwash, for the probe arrays near (purple circles) and far (blue crosses) from the step. In all cases, overwash reduces the steepness of the reflected wave, and greater reductions in steepness occur for larger ka, i.e. when deeper and faster overwash occurs. For instance, the reduction in steepness due to overwash for $ka = 0.03$ is $\sim 19\%$ and for $ka = 0.13$ is $\sim 36\%$. Hence, as expected, the reflected waves far from the step are significantly less than when no overwash occurs and the reduction increases when larger amounts of overwash occur. The results taken from probes near to ($\approx \lambda/5$) and far from ($\approx 2\lambda$) the step show almost exact agreement, with relative differences of less than 3%. This suggests that change in flow properties from deep water to shallow water flow (that occurs around the step vertex) is localised to a region of at least a fifth of the incident wave's wavelength.

The left-hand panel of figure 6 shows the amplitude of the second harmonic of the reflected wave, $r(2\omega)$, relative to the amplitude of the reflected wave at the fundamental frequency, $r(\omega)$, for varied ka. The right-hand panel shows the phase of the reflected wave at the fundamental frequency relative to the phase of the incident wave, $\theta_R(\omega)$, for varied ka. The magenta circles are results for the probe array near to the step, the blue crosses are the results for the prove array far from the step, and the dashed black line is the standing wave solution (no overwash).

The left-hand panel shows the higher-order harmonics increase with increasing incident wave amplitude, where $r(2\omega)/r(\omega) \approx 0.03$ for $a = 5\,\mathrm{mm}$ and $r(2\omega)/r(\omega) \approx 0.06$ for $a = 20\,\mathrm{mm}$. This indicates the formation of overwash creates higher-order reflection effects, which are of greater significance for higher amplitude incident waves. Nonetheless, the higher-order waves are more than an order of magnitude less than the reflected waves at the fundamental frequency. For all other frequency bins, the amplitude of the reflection was at least two orders of magnitude less than the amplitude of the reflection at the fundamental frequency (not shown). The right-hand panel shows the phase difference between the incident and reflected waves is less than 0.07 rad in all cases. Therefore, the incident and reflected waves are still approximately in-phase, even when overwash occurs.

2.3 Step overwash prediction

The first component of the model is to simulate the overwash as in [25]. The model of [25] in briefly recounted in this section for completeness. Let the water to the left of the step obey linear potential-

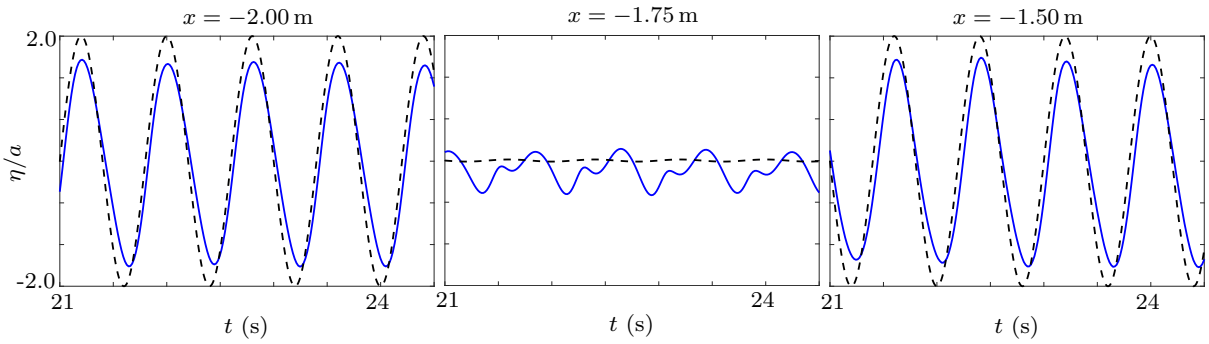

Figure 4: CFD free surface signals at locations to the left of the step once the waves become periodic, for incident wave period $T = 0.8\,\mathrm{s}$ and amplitude $a = 15\,\mathrm{mm}$. Results are shown for the case with a step (solid blue) and where the step is extended upwards such that no overwash occurs (dashed black).

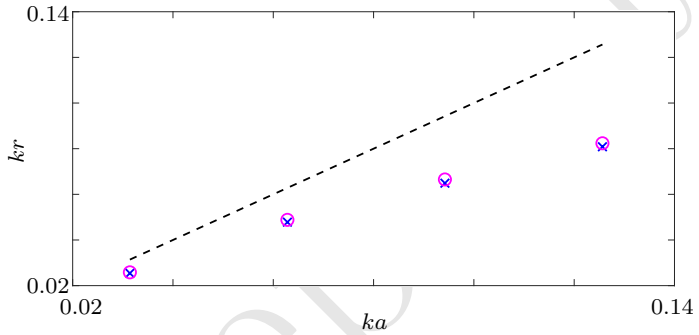

Figure 5: CFD reflected wave steepness at the fundamental frequency versus incident wave steepness. Results are shown for when no overwash occurs (dashed black) and when overwash is allowed to occur with measurements near to (magenta circles) and far from (blue crosses) the step.

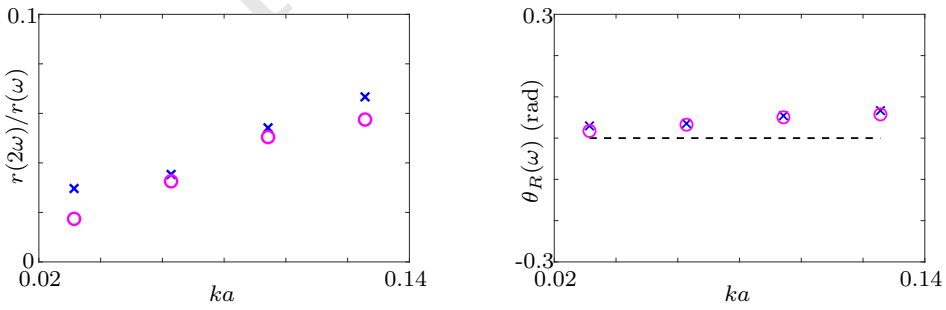

Figure 6: Left: Amplitude of the reflected wave at twice fundamental frequency divided by the amplitude of the reflected wave at the fundamental frequency versus incident wave steepness. Right: Phase difference between the incident and reflected waves at the fundamental frequency. Results are shown for when no overwash occurs (dashed black) and when overwash is allowed to occur with measurements near to (magenta circles) and far from (blue crosses) the step.

flow theory such that for $x < 0$

$$\phi(x,z,t) = \frac{g}{w}\left(a\cos(\omega t - kx) + r\cos(\omega t + kx + \theta_R)\right)\frac{\cosh(k(z+H))}{\cosh(kH)}, \tag{1}$$

where r is the amplitude of the reflected wave and θ_R is the phase of the reflected wave. Assuming, at this stage, that the overwash has no effect on the surrounding waves, all incident wave energy is reflected by the step, creating a standing wave field [12]. Thus, $r \equiv r_{lin} = a$ and $\theta_R = 0$ (where r_{lin} is given by linear potential-flow theory). The corresponding velocity field is $(u, w) = \nabla\phi$, where u and w are the x- and z-direction velocities, respectively, and the free surface is

$$\eta(x,t) = -g^{-1}\partial_t\phi(x,0,t) \quad \text{for} \quad x < 0. \tag{2}$$

The overwash is modelled using the nonlinear shallow water equations for $x > 0$. These are

$$\partial_t h + \partial_x(h\hat{u}) = 0 \quad \text{and} \tag{3a}$$

$$\partial_t(h\hat{u}) + \partial_x(h\hat{u}^2 + \frac{1}{2}gh^2) = 0, \tag{3b}$$

where $h(x,t)$ is the depth of the water on the step, and $\hat{u}(x,t)$ is the depth averaged horizontal velocity [27]. The boundary conditions at the left-hand end of the overwash are set as

$$h(x = 0^-, t) = \max(\eta(x = 0^-, t), 0) = \max(2a\sin(wt), 0) \quad \text{and} \tag{4}$$

$$\hat{u}(x = 0^-, t) = u(x = 0^-, z = 0, t) = 0. \tag{5}$$

The boundary conditions make use of the notation $x = 0^{\pm}$ to denote $x = 0$ taken from below (superscript $-$) and below (superscript $+$), i.e. the flow properties from the deep and shallow water limits of their interface. Discussion of why this is necessary is given by [25].

Far to the right of the step a boundary condition is set such that

$$h(x = F, t) = 0 \quad \text{and} \quad \hat{u}(x = F, t) = 0 \quad \text{for some } F \gg 0. \tag{6}$$

The condition simulates the overwash freely radiating outwards as $x \to \infty$, on the basis that the flow is supercritical at $x = F$, which is justified by the characteristic curves shown in figure 7 (these results are not given by [25]). On the characteristic curves $\xi_{\pm} = \hat{u} \pm 2\sqrt{gh}$ are the Riemann invariants (solid blue for negative, dashed red for positive). They are taken when the flow has become periodic in time, and for the simulation with $a = 15\,\text{mm}$. The thick jagged red lines are where characteristics of the same kind intersect, and create hydraulic jumps (bores) [27], where the jaggedness is a result of data being stored in a numerical grid. For x greater than approximately 0.15 m the characteristics always have a positive slope, so that setting, $F = 0.4\,\text{m}$ say, the flow is supercritical at the boundary $x = F$. Therefore, the flow at $x = F$ is only influenced by what has occurred downstream [4], and the flow at $x = 0^+$ is not influenced by the choice of F, which simulates the flow radiating freely as $x \to \infty$.

2.4 Naive energy correction theory

According to the shallow-water theory used to model the overwash in [25], the (density scaled) energy flux[1] in the overwash is

$$E_{ow}(x,t) = \frac{1}{2}h\hat{u}^3 + gh^2\hat{u}. \tag{7}$$

The results of [25] show that values of E_{ow} using $\hat{u}$ and h from the overwash model in §2.3 are accurate when compared to values given by a CFD model.

[1] In this paper the energy flux is defined as the flux of the kinetic and potential energy through a boundary plus the work done by pressure at the boundary. This is done for simplicity.

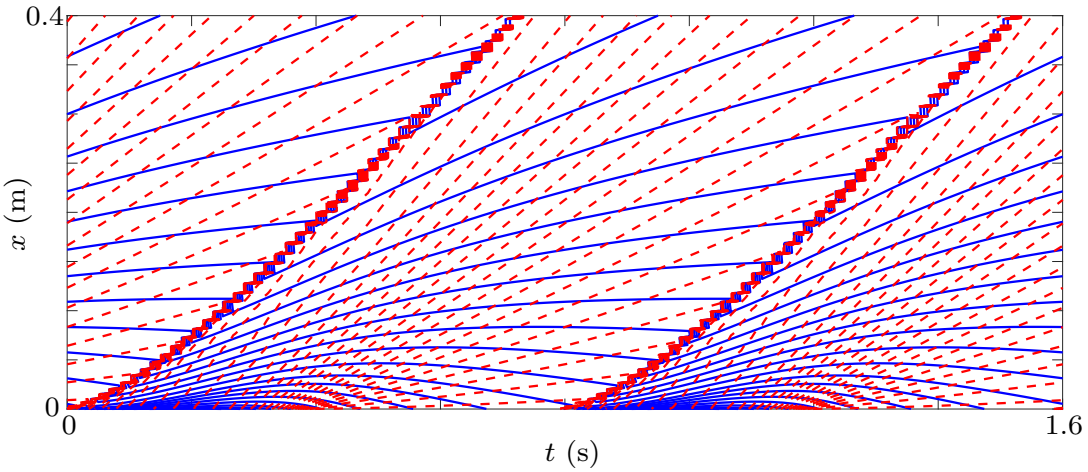

Figure 7: Characteristic curves of the invariants $\xi_- = \hat{u} - 2\sqrt{gh}$ (solid blue) and $\xi_+ = \hat{u} + 2\sqrt{gh}$ (dashed red) in the overwash for the step problem. Plot is for incident wave period $T = 0.8\,\mathrm{s}$ and amplitude $a = 15\,\mathrm{mm}$.

It would therefore seem reasonable to use the prediction of E_{ow} from the overwash model to obtain a corrected reflected wave that is consistent with the transfer of energy into the overwash. The method derived here is based on the assumption that the primary influence of the overwash formation is to change the amplitude of the reflected wave, as motivated by the findings from figures 5 and 6. Thus, it is assumed that for $x \ll 0$ the wave-field maintains the form given in equation 1 with $\theta_R = 0$, but with some as yet unknown corrected reflection amplitude $r = r_c$.

Assuming that no mechanical energy is lost in the formation of the overwash, the energy balance for (what we refer to as) the 'naive' theory is straightforward to derive, and results in

$$\frac{g^2 k}{2\omega}\left(\frac{\tanh(kH) + Hk\mathrm{sech}^2(Hk)}{2k}\right)(a^2 - r_c^2) = \overline{E_{ow}(0^+, t)}, \tag{8}$$

where $\overline{\bullet} = \frac{\omega}{2\pi}\int_{t=t_1}^{t_1+\frac{2\pi}{\omega}} \bullet \,\mathrm{d}t$ is the operator that defines averaging over a wave period. The term on the left-hand side of (8) is the energy entering from the incident wave at some $x \ll 0$ minus the energy leaving from the reflected wave [18]. The term on the right-hand side is the energy flux into the overwash. Using the deep water limit $H \gg \lambda$ (which holds for the waves tested), the energy balance (8) simplifies to

$$\frac{g^2}{4\omega}(a^2 - r_c^2) = \overline{E_{ow}} \quad \Rightarrow \quad r_c = \sqrt{a^2 - \frac{4\omega}{g^2}\overline{E_{ow}(0^+, t)}}, \tag{9}$$

where the positive branch is taken, and $E_{ow}(0^+, t)$ can be calculated from (8).

Figure 8 shows the reflected steepness versus incident steepness, as in figure 5, but with predictions given by the naive theory overlaid (dotted magenta). Although the naive method gives a better prediction for the reflected amplitude than linear theory, it over-predicts the reflected steepness observed in the CFD simulations poorly as overwash becomes more pronounced. This is particularly true for the $ka = 0.13$ case, where the error is as large as 27%. This indicates that non-negligible energy dissipation processes are present in the overwash phenomena.

2.5 Step reflection transition-loss correction theory

A likely region for energy dissipation is the interface between the deep water and shallow overwash, based on the observation from the CFD model that wave breaking and other complex (potentially

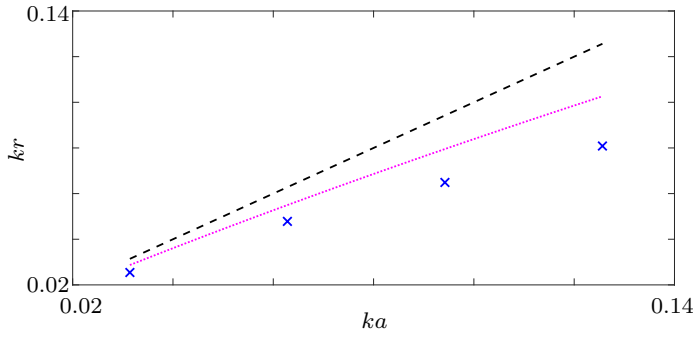

Figure 8: As in figure 5 but with the results of the naive energy method overlaid (doted magenta).

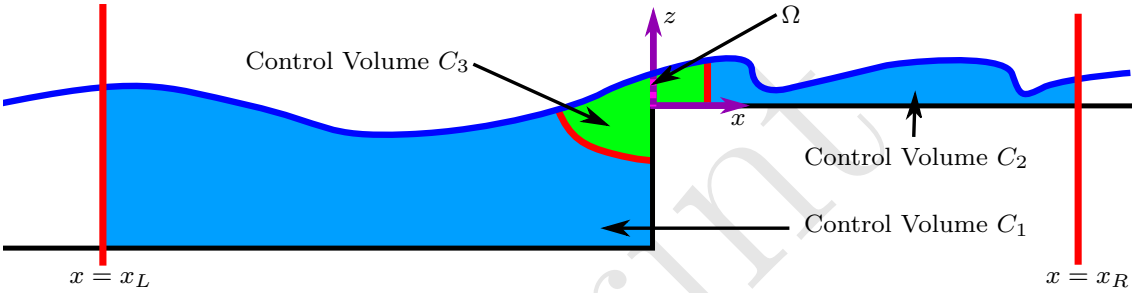

Figure 9: Schematic of step control volumes (not to scale).

dissipative) dynamics occur in this region [25]. Therefore, consider the schematic in figure 9, which shows three distinct control volumes (flow domains) that bound the water between $x_L \ll 0$ and $x_R > 0$. Control volume C_1 contains the deep water to the left of the step, excluding the portion at the interface. Control volume C_2 contains the overwash water, excluding the portion at the interface. Control volume C_3 contains the water at the interface. It is assumed that the water in C_1 obeys linear potential-flow theory, which conserves energy, and the water in C_2 obeys shallow water theory, in which energy losses occur due to bores, which can be calculated [4]. The water in C_3 contains the complicated dynamics involved in the transition between these types of flows, which is more difficult to account for.

Motivated by the analysis of figure 5, suppose the width of C_3 is small relative to the horizontal length scales of the problem (i.e. the length of the waves and bores), and that the flow transition occurs over a vertical branch at the upper vertex of the step, i.e. $C_3 \equiv \Omega = \{(x, z) : x = 0, z > 0\}$. The flow is permitted to have a discontinuity over Ω, so that a hydraulic jump may exist at the deep to shallow water interface.

Discontinuities change the usual energy conservation laws and produces energy losses. This is a well known phenomenon in, for instance, shallow water bores [4]. Using the laws outlined by [6], conservation of mechanical energy in the control volume $C = C_1 \cup C_2 \cup C_3$ with boundary ∂C is given as

$$\int_C \frac{\partial}{\partial t} E_t \, \mathrm{d}V + \int_{\partial C \setminus \Omega} (E_t + p)\mathbf{u}_r \cdot \mathbf{n} \, \mathrm{d}S + \left[\int_\Omega (E_t + p)\mathbf{u}_r \cdot \mathbf{n} \, \mathrm{d}S \right]_{x=0^-}^{x=0^+} - L_{bores} = 0, \tag{10}$$

where E_t is the kinetic and potential energy of the water, p is the pressure, $\mathbf{u}_r$ is the velocity of the flow relative to the velocity of the boundary (the boundary has a velocity of zero on all boundaries except the free surface where it equals the flow velocity), $\mathbf{n}$ is the outwards facing normal (defined as

$\mathbf{n} = (1, 0)$ on Ω), and L_{bores} is the energy dissipated by the bores in C_2. Note that the third integral on the left-hand side of (10) is the result of allowing discontinuity of the flow over the interface Ω.

By assuming the flow is periodic at the incident wave frequency and noting the relative velocity of the fluid on the free surface and basin boundaries is zero, (10) simplifies to

$$\begin{aligned} 0 = &+ \overline{\int_{-H}^{\eta} (E_t + p)u|_{x=x_L} \, \mathrm{d}z} + \overline{\int_0^{\eta^-} (E_t + p)u|_{x=0^-} \, \mathrm{d}z} \\ &- \overline{\int_0^{\eta^+} (E_t + p)u|_{x=0^+} \, \mathrm{d}z} - \overline{\int_0^{\eta^+} (E_t + p)u|_{x=x_R} \, \mathrm{d}z} - \overline{L_{bores}}, \end{aligned} \tag{11}$$

where $\eta^- = \max\{\eta(0^-, t), 0\}$ and $\eta^+ = h(x = 0^+, t)$. As bores only dissipate energy as they propagate in space [4], by taking $x_R \to 0^+$ the identity can be expressed as

$$\begin{aligned} 0 = &+ \overline{\int_{-H}^{\eta} (E_t + p)u|_{x=x_L} \, \mathrm{d}z} - \overline{\int_0^{\eta^+} (E_t + p)u|_{x=0^+} \, \mathrm{d}z} \\ &+ \overline{\int_0^{\eta^-} (E_t + p)u|_{x=0^-} \, \mathrm{d}z} - \overline{\int_0^{\eta^+} (E_t + p)u|_{x=0^+} \, \mathrm{d}z}, \end{aligned} \tag{12}$$

where the first two integrals on the right-hand side represent energy flux in/out of C, and the last two integrals represent energy dissipated over the instantaneous transition.

According to linear potential-flow theory, the pressure, energy, velocity in C_1 are

$$p = -\rho\left(\partial_t\phi + \frac{1}{2}(w^2 + u^2) + gz\right), \quad E_t = \rho\left(\frac{1}{2}(w^2 + u^2) + gz\right), \tag{13a}$$

$$\text{and} \quad \mathbf{u} = (u, w) = (\partial_x\phi, \partial_z\phi), \tag{13b}$$

whereas, in C_2, according to shallow-water theory, they are

$$p = \rho g(\eta - z), \quad E_t = \frac{\rho\, u^2}{2} + \rho g z, \quad \text{and} \quad u(x, z, t) = \hat{u}(x, t). \tag{14}$$

These identities are used to evaluate the integrals in (12), as shown in Appendix A. By neglecting the terms above order k^3a^3 (consistent with linear theory [18]), (12) becomes

$$\frac{g^2k}{2\omega}\left(\frac{\tanh(kH) + Hk\operatorname{sech}^2(Hk)}{2k}\right)(a^2 - r_c^2) + \frac{4g^2k}{6\pi\omega}(a - r_c)(a + r_c)^2 = 2\overline{E_{ow}(0^+, t)}. \tag{15}$$

Further simplifications to (15) can be made by taking the deep water approximation, which gives

$$\frac{g^2}{4\omega}(a^2 - r_c^2) = \left(\overline{E_{ow}(0^+, t)} - \frac{2g^2k}{3\pi\omega}(a - r_c)(a + r_c)^2\right) + \overline{E_{ow}(0^+, t)}. \tag{16}$$

This equation has deliberately been written in a manner to compare to the naive energy theory (9). It shows that the difference between the two methods is the first term on the right-hand side of (16), which is cubic with respect to r_c and contains one count of the energy going into the overwash. This term encapsulates energy dissipated in the transition. Therefore, the reflected wave amplitude can be calculated as the root of the cubic equation

$$\frac{g^2}{4\omega}(a^2 - r_c^2) + \frac{2g^2k}{3\pi\omega}(a - r_c)(a + r_c)^2 = 2\overline{E_{ow}(0^+, t)} \quad \text{where} \quad 0 \le r_c \le a. \tag{17}$$

The transition-loss theory predictions of the reflected steepness are compared against the linear theory, CFD data, and the naive correction theory in figure 10. The transition-loss predictions (dashed red curve) almost intersect all CFD data points. On average, the relative difference between the transition-loss theory and CFD data is 1.9%, and is only 2.5% at worst, which occurs for the steepest incident wave, $ka = 0.13$. Therefore, the transition-loss theory is a marked improvement on both the linear potential-flow theory and the naive energy-loss theory, which have errors as large as 55% and 27% for $ka = 0.13$ case, respectively.

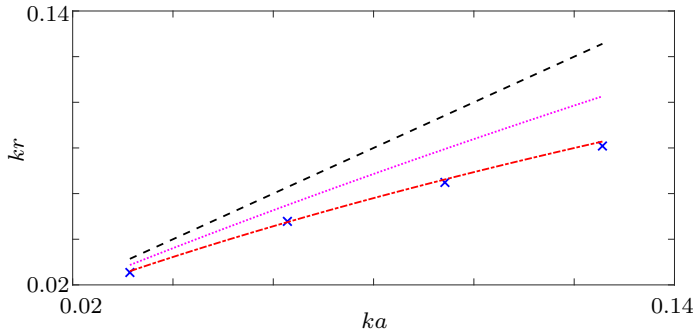

Figure 10: As in figure 8 but with the results of the transition loss energy method overlaid (dot dashed red).

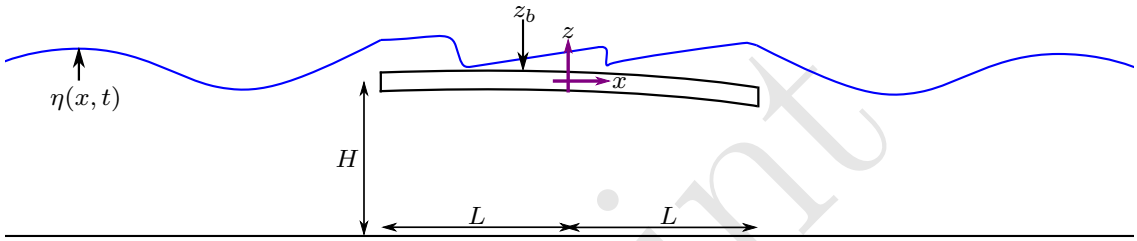

Figure 11: Schematic of plate problem (not to scale).

3 Waves transmitted by a plate

3.1 Problem description

Consider an effectively two dimensional wave basin filled with water of depth $H = 0.9\,\mathrm{m}$, as in the experiments of [21]. Locations in the basin are defined using the Cartesian coordinate system (x, z), where z points upwards and x points along the still water line. A floating elastic plate of length $2L = 1\,\mathrm{m}$ is placed in the basin, centred at $x = 0$. The basin is (effectively) infinitely long in the positive and negative x-directions, i.e. energy can radiate out freely towards these limits. The plate has thickness $s = 0.01\,\mathrm{m}$, density $\rho_p = 570\,\mathrm{kg\,m^{-3}}$, Young's modulus $E = 500\,\mathrm{MPa}$, a Poisson's ratio $\nu = 0.4$, and it is assumed that its surge and drift motion is negligible such that there is no translation about the x-axis (but the plate is still free to pitch, heave, and deform vertically). The plate is subject to regular monochromatic waves with steepness between $ka = 0.06$ and 0.15, and frequencies $\omega = 7.85$, 6.98, and $6.28\,\mathrm{rad\,s^{-1}}$ (with corresponding periods $T = 0.8$, 0.9, and 1.0 s, respectively) that propagate in the positive x-direction. The incident wave and plate parameters are consistent with a series of tests reported by [21]. A representative schematic of the system is shown in figure 11.

3.2 Plate overwash prediction

Two key assumptions are made for the plate problem to extend the methodology outlined for the step in §2.3: (i) overwash formation it is not affected by the water already on the plate; and (ii) overwash that returns to the surrounding water does not contribute wave energy at the incident frequency. Assumption (i) is motivated by the videos presented by [24], which indicate bore formation is not affected by returning overwash flow. Assumption (ii) is based on the hypothesis that the overwash

is sufficiently irregular to prevent the returning flow from creating waves at the incident frequency. The assumptions allow the overwash model of [24] to be simplified, such that it only approximates the energy flowing into the overwash, and not the overwash itself.

The flow to the left ($x < -L$) and right ($x > L$) of the plate is described using linear potential-flow theory as, respectively,

$$\phi(x,z,t) = \frac{g}{w}\left(a\cos(\omega t - kx) + r\cos(\omega t + kx + \theta_R)\right)\frac{\cosh(k(z+H))}{\cosh(kH)}, \tag{18a}$$

$$\text{and} \quad \phi(x,z,t) = \frac{g}{w}\left(\tau\cos(\omega t - kx + \theta_T)\right)\frac{\cosh(k(z+H))}{\cosh(kH)}, \tag{18b}$$

where τ and θ_T are the amplitude and phase of the transmitted wave. The values of r, τ, θ_R and θ_T are obtained by solving the standard thin elastic plate scattering problem [20]. Expressions (18a–b) neglect the evanescent waves that decay exponentially away from $x = \pm L$, consistent with [24].

Overwash is forced by the boundary conditions

$$h(x = \pm L^{\pm}, t) = \max\{\eta(x = \pm L, t) - z_b(x = \pm L, t), 0\}, \quad \text{and} \tag{19}$$

$$\hat{u}(x = \pm L^{\pm}, t) = \begin{cases} \partial_x\phi(x = \pm L, z = 0, t), & \text{if } h(x = \pm L^{\pm}, t) > 0 \\ 0 & \text{otherwise,} \end{cases} \tag{20}$$

where boundary conditions (19) are the difference between the free surface elevation, $\eta(x,t) = -g^{-1}\partial_t\phi(x, z = 0, t)$, at the plate edges $x = \pm L$, and the location of the plate upper surface, $z_b(x,t)$, which is obtained from the thin elastic plate scattering problem. Therefore, boundary conditions (20) set the (horizontal) overwash velocity at the plate edges to match the surrounding water if the surrounding water exceeds the plate upper surface, and be zero otherwise.

In order to model key assumptions (i) and (ii), energy sink boundary conditions are set (which are not used by [24]), such that

$$h(x = F_1, t) = \hat{u}(x = F_1, t) = 0 \quad \text{and} \quad h(x = F_2, t) = \hat{u}(x = F_2, t) = 0, \tag{21}$$

where $-L \ll F_1 < F_2 \ll L$, and $x = F_1$ and $x = F_2$ are sufficiently far from the plate edges that the flow is supercritical there for all t. As with the step, the points of supercriticality are such that the overwash at $x = -L^+$ and $x = L^-$ are invariant of an increase in F_1 or a decrease in F_2. The physical interpretation of (21) is that at F_1 and F_2 there is a sink such that the energy flowing through is lost from the system and also such that it does not influence the overwash formation at the plate edges. From numerical testing (not shown), it was found that it is possible to conservatively set $F_1 = -L/2$ and $F_2 = L/2$ to satisfy the supercritical flow requirements.

3.3 Plate transmission transition-loss correction theory

The transition-loss theory is formulated with E_{ow} at $x = \pm L$ treated as known from the overwash model (7). The potential surrounding the plate is given by (18), with a (as yet unknown) corrected transmitted amplitude $\tau = \tau_c$, and assuming overwash does not affect the reflected wave [21]. This contrasts with the step, where $r = r_c$ was the unknown of the problem.

Consider the schematic of the plate problem given in figure 12. Let control volume C contain the the water between $x_L \ll -L$ and $x_R \gg L$, but excluding the water on the surface of the plate between x_l and x_r, where $-L < x_l < x_r < L$. Denote the boundary of C as ∂C. As with the step, assume energy is dissipated in the transition from deep to shallow water flow, in control volumes C_L and C_R, which are sufficiently narrow they can be contracted to vertical branches $\Omega_L = \{(x,z) : x = -L, z > z_b\}$ and $\Omega_R = \{(x,z) : x = L, z > z_b\}$.

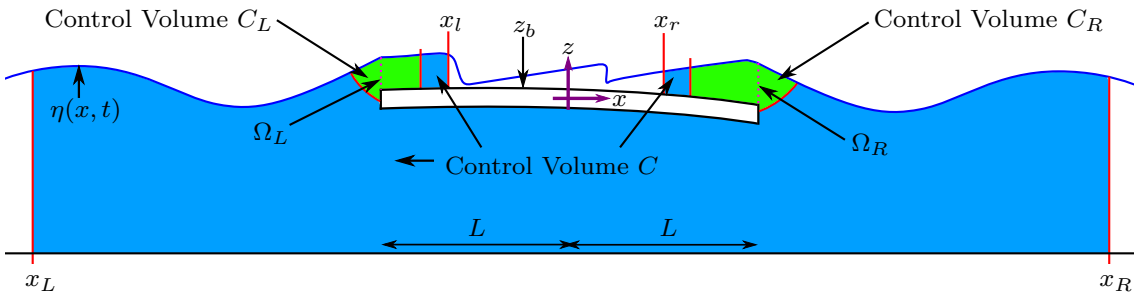

Figure 12: Schematic of plate control volumes (not to scale).

By considering the discontinuities that may occur over Ω_L and Ω_R, conservation of energy for the system is [6]

$$0 = \int_C \frac{\partial}{\partial t} E_t \,\mathrm{d}V + \int_{\partial C \setminus (\Omega_L \cup \Omega_R)} (E_t + p)\mathbf{u}_r \cdot \mathbf{n} \,\mathrm{d}S - L_{bores} + \left[\int_{\Omega_L} (E_t + p)\mathbf{u}_r \cdot \mathbf{n} \,\mathrm{d}S\right]_{x=-L^-}^{x=-L^+} + \left[\int_{\Omega_R} (E_t + p)\mathbf{u}_r \cdot \mathbf{n} \,\mathrm{d}S\right]_{x=L^-}^{x=L^+}. \tag{22}$$

Without the final two terms, (22) is the conventional description of the conservation of energy. The final two terms account for energy lost in the flow transition. As with the step problem, the L_{bores} term in this equation is the energy dissipated by the bores as they propagate over the surface of the plate, and, because they dissipate energy as they traverse space, L_{bores} becomes zero by setting $x_l = -L^+$ and $x_r = L^-$.

By enforcing the no-flow-penetration conditions on the plate boundary, the free surface, and the basin bed, (22) simplifies to

$$\begin{aligned}\int_C \frac{\partial}{\partial t} E_t \,\mathrm{d}V = &+ \int_{-H}^{\eta} (E_t + p)u|_{x=x_L} \,\mathrm{d}z - \int_{-H}^{\eta} (E_t + p)u|_{x=x_R} \,\mathrm{d}z \\ &+ \int_{z_b}^{\eta} (E_t + p)u|_{x=-L^-} \,\mathrm{d}z - \int_{z_b}^{\eta} (E_t + p)u|_{x=-L^+} \,\mathrm{d}z \\ &+ \int_{z_b}^{\eta} (E_t + p)u|_{x=L^-} \,\mathrm{d}z - \int_{z_b}^{\eta} (E_t + p)u|_{x=L^+} \,\mathrm{d}z \\ &- \int_{z_b}^{\eta} (E_t + p)u|_{x=-L^+} \,\mathrm{d}z + \int_{z_b}^{\eta} (E_t + p)u|_{x=L^-} \,\mathrm{d}z.\end{aligned} \tag{23}$$

The term on the left-hand side of (23) is the change of mechanical energy in the system. The first and second integrals on the right-hand side are the energy entering and leaving the system at the leftmost and rightmost boundaries, respectively. The third to sixth integrals on the right-hand side are the energy dissipated in the transition from deep to shallow-water flow. The final two integrals are the energy being transferred into the overwash.

Assuming all the motions in C are periodic in time, with the same period as the incident wave, the time averaged version of (23) is

$$\begin{aligned}0 = &+ \overline{\int_{-H}^{\eta} (E_t + p)u|_{x=x_L} \,\mathrm{d}z} - \overline{\int_{-H}^{\eta} (E_t + p)u|_{x=x_R} \,\mathrm{d}z} + \overline{\int_{z_b}^{\eta} (E_t + p)u|_{x=-L^-} \,\mathrm{d}z} \\ &- 2\overline{\int_{z_b}^{\eta} (E_t + p)u|_{x=-L^+} \,\mathrm{d}z} + 2\overline{\int_{z_b}^{\eta} (E_t + p)u|_{x=L^-} \,\mathrm{d}z} - \overline{\int_{z_b}^{\eta} (E_t + p)u|_{x=L^+} \,\mathrm{d}z}.\end{aligned} \tag{24}$$

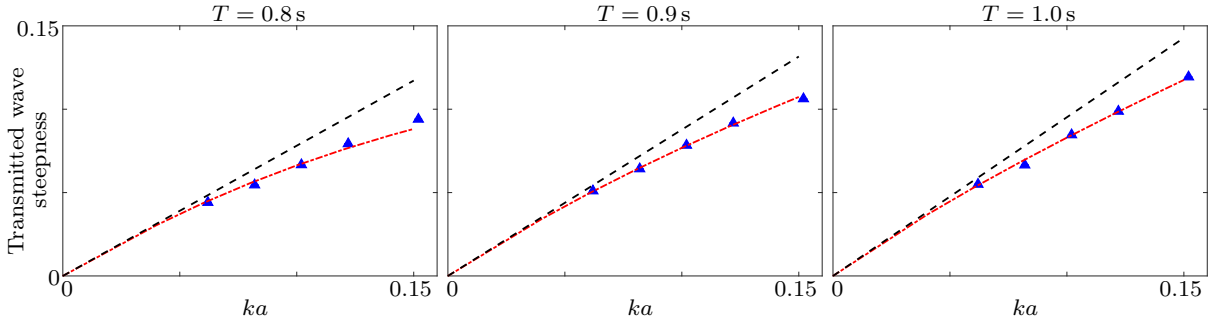

Figure 13: As in figure 1 but with transition-loss theory predictions overlaid in dot dashed red.

Using the wave-field ansatz (18) and flow properties (13), the integrals at $x = x_L$ and $x = x_R$ are evaluated to give

$$\frac{g^2\rho}{4\omega}(-a^2 + r^2 + \tau_c^2) = +\overline{\int_{z_b}^{\eta}(E_t + p)u|_{x=-L^-}\,\mathrm{d}z} - \overline{\int_{z_b}^{\eta}(E_t + p)u|_{x=L^+}\,\mathrm{d}z} \\ +2\overline{\int_{z_b}^{\eta}(E_t + p)u|_{x=L^-}\,\mathrm{d}z} - 2\overline{\int_{z_b}^{\eta}(E_t + p)u|_{x=-L^+}\,\mathrm{d}z}, \tag{25}$$

where, as for the analogous step problem identity in (16) deep water conditions have been applied, and terms $O(k^4a^4)$ or greater have been neglected.

It is assumed $u \approx 0$ for $x = \pm L^{\pm}$ and $z \in (z_b(\pm L^{\pm}, t), \eta(z_b(\pm L^{\pm}, t))$, on the basis $u = 0$ on the vertical plate edges, and hence the first two integrals on the right-hand side of (25) vanish. Further, similar to the step problem, the overwash at the edges of the plate is assumed to be described well by the shallow-water equations, such that the final two integrals can be evaluated, and (25) becomes

$$\frac{g^2}{4\omega}\tau_c^2 = \frac{g^2}{4\omega}(a^2 - r^2) - 2\overline{E_{ow}(-L^+, t)} + 2\overline{E_{ow}(L^-, t)}. \tag{26}$$

This states the reduction in energy of the transmitted wave due to overwash is double the energy entering the overwash, where energy reduction is due to both energy entering the overwash and energy loss in the transition from deep water waves to shallow-water flow. Therefore, the transmitted wave amplitude is

$$\tau_c = \sqrt{(a^2 - r^2) - \frac{8\omega}{g^2}\overline{E_{ow}(-L^+, t)} + \frac{8\omega}{g^2}\overline{E_{ow}(L^-, t)}}, \tag{27}$$

where $E_{ow}(-L^+, t)$ and $E_{ow}(L^-, t)$ are calculated from the overwash model.

Figure 13 shows transition-loss theory predictions of the transmitted wave steepness, $k\tau_c$, overlaid (dot dashed red) on figure 1, i.e. the experimental results of [21] (blue squares), and with linear potential-flow theory for reference (solid black). The transition-loss theory shows the same sub-linear trend as the experimental measurements and is very close to the experimental measurements for all steepnesses, ka, and wave periods, T. The agreement is best for wave period $T = 1.0\,\mathrm{s}$, where the transition-loss theory differs from the experiments by 2.3% on average, and is always within 3.9%. The largest error, 6.2%, occurs for for $T = 0.8\,\mathrm{s}$ and $ka = 0.15$, but despite this the average error is only 2.8% for $T = 0.8\,\mathrm{s}$. The transition-loss predictions are marked improvements on the linear theory; especially for the highest steepness waves, $ka = 0.15$, where the transition-loss theory agrees with the experiments on average by 2.9%, compared to the linear theory average difference of 22.8%.

4 Conclusions

Reflection on regular incident waves by an overwashed step and transmission by an overwashed plate have been investigated, and transition-loss theories were proposed to calculated reflected and transmitted wave amplitudes. For the overwashed step problem, the CFD model of [25] was used to analyse the waves reflected by the step. As anticipated by the related overwashed floating plate literature, the occurrence of overwash was found to significantly reduce reflected wave amplitudes. Reflected waves at frequencies different to the incident wave frequency were observed when overwash occurred, but the corresponding amplitudes were shown to be small in comparison to the amplitude of the linear component (i.e. the reflected wave component at the incident wave frequency dominates the reflected field). It was shown that the reduced amplitudes cannot be accounted for by flux of energy into the overwash alone, but, rather, a combination of the flux into the overwash and mechanical energy dissipated in transition from deep water to shallow water should be considered. The transition-loss theory was based on the assumptions that the energy flux into the overwash is lost from the surrounding waves, and the mechanical energy dissipated by the transition from deep water waves to shallow-water flow occurs over a sufficiently small domain that it can be modelled as a discontinuity in the flow (akin to a hydraulic jump). The theoretical predictions of the reflected wave amplitudes were shown to be in excellent agreement with amplitudes extracted from CFD data.

A transition-loss theory for transmission by the plate was derived using a similar methodology to the step problem, but with the experimentally motivated assumption that the overwashed plate reduces wave transmission and does not affect reflection. The predictions showed strong agreement with experimental measurements, and were shown to be a significant improvement over linear theory.

This work has considered overwash problems in two dimensions that are forced by regular waves. It remains unclear how the theory can be extended to include a third spatial dimension, irregular waves, and more complicated plate geometries or motions (e.g. drift motions). Such work will likely require additional experimental testing to for these extended cases; although the principle idea developed in this paper of overwash dissipating energy though formation of a shallow-water flow and removal of energy within the shallow-water flow may remain valid.

A Evaluation of energy integrals

Consider

$$I_1 = \overline{\int_{-H}^{\eta} (E_t + p)u|_{x=x_L} \, \mathrm{d}z}. \tag{28}$$

Through the identities of (13) and a Taylor expansion about the free surface this gives [18]

$$\frac{I_1}{\rho} = \overline{\int_{-H}^{0} -\partial_t\phi\partial_x\phi|_{x=x_L} \, \mathrm{d}z} + O(k^4a^4). \tag{29}$$

Keeping this equation accurate to (at least) third order with respect to ka, this implies

$$\frac{I_1}{\rho} \approx \frac{g^2k}{2\pi} \int_0^{\frac{2\pi}{\omega}} \left(a^2\sin^2(\omega t - kx_L) - r^2\sin^2(wt + kx_L)\right) \mathrm{d}t \times$$

$$\int_{-H}^{0} \frac{\cosh^2(k(z+H))}{\cosh^2(kH)} \, \mathrm{d}z \tag{30}$$

$$= \frac{g^2k}{2\omega} \left(\frac{\tanh(kH) + Hk\mathrm{sech}^2(Hk)}{2k}\right) \left(a^2 - r^2\right). \tag{31}$$

Additionally, consider

$$I_2 = \overline{\int_0^{\eta^-} (E_t + p)u|_{x=0^-} \, \mathrm{d}z}. \tag{32}$$

Through the identities of (13) and a Taylor expansion about the free surface it can be shown that this implies

$$\frac{I_2}{\rho} = \overline{-\eta^- \partial_t \phi(0,0,t) \partial_x \phi(0,0,t)} + O(k^4 a^4). \tag{33}$$

Keeping this equation accurate to (at least) third order with respect to ka, this implies

$$\frac{I_2}{\rho} \approx \frac{g^2 k}{\omega} \frac{\omega}{2\pi} \int_0^{\frac{2\pi}{\omega}} \left(a^2 \sin^2(\omega t) - r^2 \sin^2(\omega t)\right) \max\left\{a \sin(\omega t) + r \sin(\omega t), 0\right\} \, \mathrm{d}t \tag{34}$$

$$= \frac{2g^2 k}{3\pi\omega}(a - r)(a + r)^2. \tag{35}$$

Finally, consider

$$I_3 = \overline{\int_0^{\eta^+} (E_t + p)u|_{x=0^+} \, \mathrm{d}z}. \tag{36}$$

Using the identities of (2.5) this can be written as

$$\frac{I_3}{\rho} = \overline{\int_0^{\eta^+} \left(\frac{1}{2}\hat{u}^3 + g\eta\hat{u}\right)_{x=0^+} \mathrm{d}z} \tag{37}$$

$$= \overline{\left(\frac{1}{2}h\hat{u}^3 + gh^2\hat{u}\right)_{x=0^+}} = \overline{E_{ow}(0^+, t)}. \tag{38}$$

Acknowledgments

CFD model data from [25] was provided by Kevin Maki and Michael Wright (University of Michigan). Experimental data from [21] was provided by Filippo Nelli and Alessandro Toffoli (University of Melbourne).

References

[1] L. G. Bennetts, A. Alberello, M. H. Meylan, C. Cavaliere, A. V. Babanin, and A. Toffoli, *An idealised experimental model of ocean surface wave transmission by an ice floe*, Ocean Model., 96 (2015), pp. 85–92.

[2] L. G. Bennetts and V. A. Squire, *On the calculation of an attenuation coefficient for transects of ice-covered ocean*, Proc. Roy. Soc. A, 468 (2012), pp. 136–162.

[3] L. G. Bennetts and T. D. Williams, *Water wave transmission by an array of floating discs*, Proc. Roy. Soc. A, 471 (2015), p. 20140698.

[4] J. Billingham and A. C. King, *Wave motion*, Cambridge university press, 2000.

[5] B. Buchner, *Green water on ship-type offshore structures*, PhD thesis, Delft University of Technology Delft, The Netherlands, 2002.

[6] J. Casey, *On the derivation of jump conditions in continuum mechanics*, The International Journal of Structural Changes in Solids, 3 (2011), pp. 61–84.

[7] A. Dolatshah, F. Nelli, L. G. Bennetts, A. Alberello, M. H. Meylan, J. P. Monty, and A. Toffoli, *Hydroelastic interactions between water waves and floating freshwater ice*, Phys. Fluids, 30 (2018), p. 091702.

[8] M. Greco, G. Colicchio, and O. Faltinsen, *Shipping of water on a two-dimensional structure. part 2*, J. Fluid Mech., 581 (2007), p. 371.

[9] M. Greco, O. M. Faltinsen, and M. Landrini, *Shipping of water on a two-dimensional structure. part 1*, J. Fluid Mech., 525 (2005), p. 309.

[10] J. Grue, *Nonlinear water waves at a submerged obstacle or bottom topography*, J. Fluid Mech., 244 (1992), pp. 455–476.

[11] L. Huang, K. Ren, M. Li, Z. Tukovi, P. Cardiff, and G. Thomas, *Fluid-structure interaction of a large ice sheet in waves*, Ocean Engineering, 182 (2019), pp. 102–111.

[12] H. Lamb, *Hydrodynamics*, Cambridge university press, 1895.

[13] C. M. Linton and P. McIver, *Handbook of mathematical techniques for wave/structure interactions*, CRC Press, 2001.

[14] E. P. D. Mansard and E. R. Funke, *The measurement of incident and reflected spectra using a least squares method*, in 17th International Conference on Coastal Engineering, 1980, pp. 154–172.

[15] R. A. Massom and S. E. Stammerjohn, *Antarctic sea ice change and variability - Physical and ecological implications*, Polar Science, 4 (2010), pp. 149–186.

[16] G. J. McCauley, H. Wolgamot, S. Draper, and J. Orszaghova, *Wave interaction with a shallowly submerged step in 2d*, in International Conference on Offshore Mechanics and Arctic Engineering, American Society of Mechanical Engineers, 2019.

[17] D. J. McGovern and W. Bai, *Experimental study on kinematics of sea ice floes in regular waves*, Cold Reg. Sci. Tech., 103 (2014), pp. 15–30.

[18] C. C. Mei, M. Stiassnie, and D. K.-P. Yue, *Theory and applications of ocean surface waves: Nonlinear aspects*, vol. 23, World scientific, 2005.

[19] M. H. Meylan, L. G. Bennetts, C. Cavaliere, A. Alberello, and A. Toffoli, *Experimental and theoretical models of wave-induced flexure of a sea ice floe*, Phys. Fluids, 27 (2015), p. 041704.

[20] M. H. Meylan and V. A. Squire, *The response of ice floes to ocean waves*, J. Geophys. Res., 99 (1994), pp. 891–900.

[21] F. Nelli, L. G. Bennetts, D. M. Skene, J. P. Monty, J. H. Lee, M. H. Meylan, and A. Toffoli, *Reflection and transmission of regular water waves by a thin, floating plate*, Wave Motion, 70 (2017), pp. 209–221.

[22] F. Nelli, L. G. Bennetts, D. M. Skene, and A. Toffoli, *Water wave transmission and energy dissipation by a floating plate in the presence of overwash*, J. Fluid Mech., 889 (2020).

[23] J. Orszaghova, A. G. Borthwick, and P. H. Taylor, *From the paddle to the beach—A Boussinesq shallow water numerical wave tank based on Madsen and Sørensen's equations*, J. Comp. Phys., 231 (2012), pp. 328–344.

[24] D. M. Skene, L. G. Bennetts, M. H. Meylan, and A. Toffoli, *Modelling water wave overwash of a thin floating plate*, J. Fluid Mech., 777 (2015).

[25] D. M. Skene, L. G. Bennetts, M. Wright, M. Meylan, and K. J. Maki, *Water wave overwash of a step*, J. Fluid Mech, 839 (2018), pp. 293–312.

[26] D. K. K. Sree, A. W.-K. Law, and H. H. Shen, *An experimental study on the interactions between surface waves and floating viscoelastic covers*, Wave Motion, 70 (2017), pp. 195–208.

[27] W.-Y. Tan, *Shallow water hydrodynamics: Mathematical theory and numerical solution for a two-dimensional system of shallow-water equations*, Elsevier, 1992.

[28] A. Toffoli, L. G. Bennetts, M. H. Meylan, C. Cavaliere, A. Alberello, J. Elsnab, and J. P. Monty, *Sea ice floes dissipate the energy of steep ocean waves*, Geophys. Res. Lett., 42 (2015), pp. 8547–8554.

[29] L. J. Yiew, L. G. Bennetts, M. H. Meylan, B. J. French, and G. A. Thomas, *Hydrodynamic responses of a thin floating disk to regular waves*, Ocean Model., 97 (2016), pp. 52–64.

[30] N. Zhang, X. Zheng, and Q. Ma, *Study on wave-induced kinematic responses and flexures of ice floe by smoothed particle hydrodynamics*, Computers & Fluids, 189 (2019), pp. 46–59.

[31] X. Zhang, S. Draper, H. Wolgamot, W. Zhao, and L. Cheng, *Eliciting features of 2d greenwater overtopping of a fixed box using modified dam break models*, Appl. Ocean Res., 84 (2019), pp. 74–91.